

Kuiperian Objects and Wandering Cosmic Objects.

by

Gilles Couture

Département des Sciences de la Terre et de l'Atmosphère

Université du Québec à Montréal

CP 8888, Succ. Centre-Ville

Montréal, QC, Canada, H3C3P8

(couture.gilles@uqam.ca)

Abstract

We study the effects of an encounter between a wandering cosmic object (WCO) of 0.1 solar mass and some Kuiperian Objects (KO). First, we let the WCO cross the out-skirt of our Kuiper belt. Such encounters can produce two types of solar objects: Eccentric Kuiper Objects of type I (EKO-I) whose perihelion is comparable to, but always smaller than the aphelion of the initial KO and Eccentric Kuiper Objects of type II (EKO-II) whose perihelion can be as small as a few AU. EKO-I tend to have a fairly large range of eccentricities, but EKO-II tend to have very large eccentricities. Both tend to be produced in clusters similar to those observed in Extreme TransNeptunian Objects (ETNO).

When a WCO crosses the path of an EKO-I, it will produce two main classes of objects: Far Kuiper Objects (FKO) of types I and II. The Sednitos discovered in the past years fit the FKO-I class with their large major axis and fairly large eccentricity, while the FKO-II class is different with its large major axis but smaller eccentricity and opposite spinning direction. When a WCO encounters an EKO-II, the latter can remain in the same class, spinning in either direction, it can end up in the EKO-I class also spinning in either direction, but it can also be sent onto orbits with extremely long semi-major axis, relatively small eccentricity where both spins are allowed. This FKO-III class could be likened to Lower Oort Cloud Objects as their major axis is a fair fraction of a light-year.

These results lead us to consider the possibility that the Kuiper Belt was once substantially larger than it is now, perhaps 90 AU. We find some evidence of this scenario in current astronomical data.

Introduction

The Kuiper Belt is a very complicated dynamical system whose current configuration likely carries traces of the genesis of the solar system. Its different populations [Gladman et al., 2008] have been influenced by the early solar environment and it has been shown [Ida *et al.* 2000] that their orbital distributions present evidence of interactions with neighbour stars similar to the Sun at this early epoch. Several models of genesis have been tested with ever increasing numbers of elements [Gladman et al., 2001, Morbidelli et al. 2007, Morbidelli & Nesvorny, 2019]. Interestingly, among the different populations, it seems binary systems are in fact fairly common and play an important role. [Thirouin, Sheppard & Noll, 2017, Thirouin & Sheppard, 2018, Fraser et al., 2017] Once a population is created, its evolution will be subjected to its environment. Complex resonances coupling elements of the Kuiper belt to our giant planets have been observed over the past decades [Bannister et al. 2016; Holman et al. 2017] indicating clearly that they have played a role in shaping the belt. Multiple simulations [Levison et al. 2007, Brasser & Morbidelli, 2013] over the years have shown that the fate of planetesimals can be dramatic in an open clusters where stars are formed: they can be exchanged between stars or even ejected altogether [Hands et al., 2019]. The early environment of the sun has implications as far away as the inner Oort cloud system [Brasser et al., 2011]

A recent global survey [Bannister *et al.*, 2018] has provided a wealth of information that will not only constrain these models but also constrain the populations of objects that lay beyond the Kuiper belt as they would affect the Kuiperian elements [Kaib et al. 2019]. Interestingly, the population of craters observed recently on Pluto and Charron by New Horizon [Singer, K.N., 2019] seems to indicate a deficit in the population of small objects in the Kuiper belt.

It has been observed that the Kuiper belt has a rather sharp edge at about 50AU.[Allen et al., 2001] The origin of this edge is still not well understood but some stellar flyby could have played a role in its creation [Kenyon & Bromley, 2004] Beyond the edge, exists a population of elements whose eccentricities are far larger than those of the main belt. These elements are still under Neptune's influence when at their perihelion and interactions between them could be at play in producing their very different orbits. Different models were proposed to try to understand the production of these objects [Morbidelli et al. 2004; Trujillo & Brown, 2001]

Beyond these objects lay the elements that are not affected by Neptune, their perihelion being over 60 AU [Gomes et al. 2008, Brasser & Schwamb, 2015]. The first one to be discovered was Sedna [Brown, Trujillo, & Rabinowitz, 2004]. A previous object (200CR105) had already attracted a fair amount of attention because of its large aphelion. Gladman et al., (2002) had shown that it could not be a regular member of the scattered disk that had its orbit modified by direct gravitational scattering off any giant planet. Morbidelli and Levison (2004) proposed some scenarios that involved different massive objects at different epochs of the solar system or the passage of nearby stars in order to explain its orbital parameters and applied the same scenarios to 2003VB12 (Sedna). For a little while Sedna was alone in its class but the discovery of 2012VP113 brought a

second member. [Trujillo & Sheppard, 2014]. In the course of these studies, it was noticed that the distribution of these objects in space was unusual: several had a tendency to aggregate in a relatively small portion of the sky. This was explained by one [Trujillo & Sheppard, 2014] or more [de la Fuente Marcos & de la Fuente Marcos, 2014] heavier trans-Plutonian planets. Numerical simulations were later performed and the Planet Nine (NP) hypothesis was proposed [Batygin & Brown, 2016]. In order to be able to shepherd these objects in a small part of the solar system, this massive object would need a mass of about 16 Earth masses, and an orbit of comparable eccentricity (about 0.6) with an aphelion of about 120 AU. Current planetary models allow an estimate of its structure [Linder & Mordasini, 2016].

Shortly after NP was suggested, a fairly large section of its orbit was ruled out through a careful analysis of Cassini data; although very far from us, NP would have a small effect on Saturn [Fienga, A., et al., 2016]. A mean motion resonance mechanism between NP and other Sednitos was suggested as the source of the clustering of the Sednitos' orbits [Batygin & Brown, 2016] and more detailed studies followed [Malhotra et al., 2016; Millholland & Laughlin, 2017]. The effect of NP on the mass distribution within the Kuiper belt has been calculated [Lawler et al., 2016] and while the distributions with and without NP are qualitatively different, it could be very difficult to distinguish them observationally.

The recent discovery of 2015TG387 [Sheppard, Trujillo, Tholen & Kaib, 2019] brought a third member to the group of Neptune-free objects. We will also include 2013SY99 in the same category as Sedna because of its large perihelion [Barrister et al., 2017] It is still difficult to understand how these objects got to such large orbits. Were they formed at such distances from the sun or were they formed much closer and then moved far away ? If they were moved far away, what process was involved [Stern, 2004]? Could this process have moved many more of these objects ? The stellar flyby that could have shaped the edge of the Belt could also have sent objects on these exotic orbits [Kenyon & Bromley, 2004]. One potential problem with a stellar flyby is that if a star came close to our solar system in the past, it is very likely that we would have discovered it by now as a star with very little angular motion. Unless the process took place during the genesis of the solar system in which case the companion stars of the sun might be very, very far away.

The hypothesis of a ninth planet is still debated and will remain so until NP is discovered. It has been argued that the orbits of some Sednitos have been wrongly estimated, thereby weakening the reason to invoke NP at all.[Shankman et al., 2017]; although recent results tend to agree with the presence of a ninth planet [de la Fuente Marcos et al. 2017] There is also the scenario where all Sednitos were captured by the sun during a close encounter with a star and its own planets [Jilkova et al., 2015]. Batygin & Morbidelli (2017) have studied the possibility that some distant KO be trapped in some resonances with NP while Sheppard & Trujillo (2016) note that correlations among several extreme eccentric objects is further evidence of a distant massive planet. The discovery of 2015BP519 [Becker et al., 2018] was seen as further proof of its existence

because it can produce objects with orbits highly inclined with respect to the global orbital plane. Recent work however [de la Fuente Marcos et al., 2018b] warns of some caution when using 2015BP519 as further proof of the existence of PN because it appears as a statistical outlier.

Recently, a cosmic messenger has been discovered: Oumuamua.[Bacci et al., 2017, Meech et al. 2017] This object is also very special because it is believed [Bannister et al, 2017b; Knight et al. 2017; Meech et al. 2017b] to be the first interstellar planetesimal that we see. Its discovery is taken as a clue that such objects must be fairly common (at least not so rare) in interstellar space. [Pfalzer & Bannister., 2019]

Five years ago [Scholz, 2014], a faint binary system consisting of a small red dwarf and a smaller brown dwarf with masses of about 8% and 6% of a solar mass was discovered and named WISE J072003.20-084651.2. About two years later, careful measurements [Mamajek et al. 2017] showed a very small angular motion that indicates that this star was at some point in the past very close to our solar system. It is estimated that Sholz's star is now about 20 LY from us and from its speed of about 100 km/sec, it came within about 0.75 LY from our solar system about 70000 years ago. Albeit small, this system seems to have had some effect on the transients observed in our extended solar system [de la Fuente Marcos, de la Fuente Marcos, Aarseth, 2018]. The origin of this particular WS is still not well understood, but there are some ways to produce a wandering stars: a double star system that gets too close to a cluster within a galaxy and is broken up by tidal forces, a double star system that gets too close to a black hole at the center of a galaxy and loses a member to the black hole. One could also think of a star being ejected from its home galaxy during an encounter with another galaxy, and, not being able to catch up with the visiting galaxy ends up as a wandering star.

Similar to the observation of Oumuamua, one could take the observation of Schulz's star as a clue that such lone, very light stars might not be so rare in the cosmos.

In this paper, we want to quantify the effects of the passage of a wandering cosmic object (WCO) on objects that are on the outskirts of our Kuiper belt. We will choose the WCO as rather light, 0.1 solar mass, so as to be barely a star and almost invisible. If a star would have passed close to our solar system, we would have seen it already. Therefore, in order for this object to not have been detected, it must be very dim, while being relatively massive in order to have an effect on the outer solar system when it passes by. A light star seems the most appropriate object. Although an object of about one solar mass would also be possible as a light white dwarf, a light neutron star or a very small black hole, the light star seems the less exotic scenario. One could also think of a collection of several small objects (each one with a mass of a few percent of a solar mass) but this scenario seems less likely as the cluster might have been pulled apart on its journey, similar to the Shoemaker-Levy comet of 1994. Regarding its speed, we chose 50 km/sec. This value is less than the estimated speed of Scholtz's star but higher than that of Oumuamua which is estimated at 25 km/sec. We also do not want to perturb too much the objects of our Kuiper belt and our

way of achieving this is to assume that the wandering cosmic object will barely meet the out-skirt of the belt. This way, it could potentially encounter several objects that it could send to another orbit and also eject several objects in outer space, while leaving most of the Kuiper belt unaffected. Such an object has no effect on the inner solar system and very little effect on the outer planets.

In a first section, we will describe the procedure that we used to produce the three body system. Then, we will briefly describe the 3 sections of our calculations: the interaction of the CWO with the out-skirt of the Kuiper Belt and then the interaction of the CWO with two objects produced by the first interaction. The figures that we present in the paper are the regular $x - y$ plane with units in m . They are complemented by tables where we give precise values of the orbital parameters; these are tables 2, 3, and 4. In the first table, we present the orbital parameters of some Trans-Neptunian and Extreme-Trans-Neptunian objects; we categorize them as Class-I, II, and III. This is not the regular classification used for these objects [Sheppard et al. 2019], but it is relevant for the orbits produced in the process studied here. We do not include 2018VG18 in our list since its orbital parameters are not very well known yet. Note also that we include 2013SY99 in the Class-III objects (as opposed to Class-I) because of its perihelion of 50 AU, which is very close to the outer edge of the Kuiper Belt.

Calculations

The calculation was performed as follows. We have an absolute frame of reference where we put the Sun, Kuiperian object, and CWO. Our input parameters are the masses, initial coordinates, and velocities of the 3 objects. The initial coordinates of the objects are $(0, 0)$ for the sun, $(q, 0)$ for the Kuiperian object and (x_0, y_0) for the CWO. The sun is initially at rest. As for the Kuiperian object, once we decide the value of q and ε (eccentricity) its speed is calculated at $t = 0$. As for the CWO, we specify its initial position and velocity (in most cases, its velocity will be 50 km/sec) depending at what point we want it to meet the Kuiperian object. Once these initial parameters are defined, we use a few analytical time steps to start the motion properly and then we let the system evolve using $\vec{F} = m\vec{a}$ for a time step that is as small as possible. Depending on the orbits, our time step could be as large as 200-300 seconds and as small as 10 seconds. Once the calculation is done in the absolute frame, we simply bring back all coordinates and speeds in the frame of the sun, since this is our reference frame: in the figures presented here, the sun is always at the origin. When we use the absolute frame, we see that the sun moves and the path of the CWO is not a straight line.

Kuiper belt

In this calculation, we neglect the mass of the Kuiper belt and consider only the interactions between a member of the belt, the sun and the CWO. At 10^{10} kg for our KO, one could argue that this mass is very small and some objects could have a much larger mass. We have verified that we can push this mass up to 10^{20} without affecting our results; as long as the mass of the KO remains

negligible in front of a solar mass, our results hold.

We take the Kuiper belt as a disk with inner radius q_K and outer radius Q_K where the sun is at the center, the origin of our axes. The Kuiperian objects move along ellipses of small eccentricities within the disk and we make them rotate counter-clockwise always starting on the $x - axis$. Now, let a straight line cut this disk vertically but not too far from the edge; the minimal distance from this line to the center is a little smaller than Q_K . The entrance and exit points are A and B, respectively. Assume the CWO follows this straight line upward and comes from the bottom. If it crosses the disk left of the center, it will encounter the Kuiperian objects in a head-on collision with points A and B while if it crosses the disk on the right of the center, we will have a rear-end collision with entrance and exit points as C and D.

In order to see clearly the dynamics of the process, we will allow our CWO to cut the Kuiper Belt at a fair distance from the edge. Afterwards, we will see what happens when it is allowed to meet the belt at a grazing angle.

Head-on collision

Entrance point, A

We will use a KO with $q = 7.6 \times 10^{12}m$ and an eccentricity of 0.043, which leads to $Q = 8.28296 \times 10^{12}m$. We will let the WCO start its journey at initial coordinates $(-7.8 \times 10^{12}, y_0)$ and velocity $(0, 50000)$ m/sec. Then we let the system evolve. The CWO is not deflected much by the sun and comes closest at a distance of about 7.742×10^{12} m. We simply chose the initial distance y_0 depending where we want it to encounter the Kuiperian object. On Figure 1-A and Table 2, we show several orbits such an encounter can produce. The initial orbit is the ellipse in dotted black at the center. Each orbit is the result of a particular encounter: the order of decreasing-increasing minimal distance between the KO and the CWO is red-green-dark/blue(dotted)-magenta-light/blue-black. As the encounter gets closer, the orbit is pulled down from the initial orbit to the red orbit. Then, it becomes a highly eccentric orbit (green) as the minimal distance decreases before it produces less eccentric orbits as the minimal distance increases again and finally has smaller effect on the orbit as the minimal distance is fairly large. It is important to note that all these orbits are rotating counter-clockwise, (as the initial orbit) are closed, some extend very far, as can be seen in Table 2, where the angle θ_x is defined as the angle of Q (taken as vector from the sun to the aphelion) with respect to the positive $x - axis$. In these encounters, the highly eccentric orbits (green dots) are produced not by sending the KO toward the sun, but by sending it first in outer space. Also important and not shown here is that a whole class of open orbits are sent first towards the sun before being ejected; some get very close to the sun, and some are even ejected on a clockwise open orbit. These orbits happen between the green and dark-blue orbits on this figure.

We see that the window to produce highly eccentric orbits (EKO-II) is rather small compared to that for producing less eccentric orbits (EKO-I). We also see that the orbits have a tendency to cluster, both the EKO-I and the EKO-II, albeit at different angles. One must note also that it is impossible to

produce an object such that $q > Q_{initial}^{kuiper}$.

Exit point, B

On its way to the exit point, the effects of the CWO are similar to that of the black curve on Figure 1-A. Of course, this depends on the entrance and exit points: as A and B are more separated, there will be a window where the effect of the CWO will be very small, as it is farther and farther away from the KO on its journey from the entrance to the exit point.

On Figure 1-B and Table 2, we use the same colour code for the decrease-increase of the impact parameter between the CWO and the KO as for the entrance point. The initial orbit is the black-dotted ellipse in the center. As the WCO gets closer to the KO, it will drag the orbit and bring it to the red orbit. As the impact parameter decreases, the orbits will turn into very elongated orbits with small q (green) However, contrary to the entrance collision, the KO is now sent first toward the sun. As the impact parameter increases, the collision produces the not so eccentric orbits with fairly large values of Q (dark-blue and magenta) before leaving the system and producing orbits light blue and black. Again, there is a whole class of orbits that are sent toward the sun, some end up very close to the sun and can even change rotation. These orbits happen between the highly elliptical orbits (green) and the not so elliptical ones (dark blue) Again, all these orbits were ejected from the solar system.

As for the entrance point, we see that the window for producing EKO-II is rather small and it is impossible to produce an object such that $q > Q_{initial}$. Again, both EKO-I and EKO-II have a tendency to cluster. In this configuration, the angles between the two EKO-I clusters (entrance and exit) is about 170 degrees and that between the two EKO-II clusters is about 120 degrees. Note also that the two clusters are on either side of the incoming trajectory of the CWO.

In general, the CWO will get closer to the KO in an encounter that will produce an EKO-II than it will in one that will produce an EKO-I. If the CWO gets too close, the KO will be simply ejected from the solar system.

Rear-end collision

Entrance point, C

We use the same KO, (*ie* $q = 7.6 \times 10^{12}m$ and $Q = 8.283 \times 10^{12}m$) but since it is now the rear-end collision scenario, we will use the following initial coordinates for the WCO ($7.1 \times 10^{12}, y_0$) and velocity (0, 50000) m/sec, and we vary y_0 to get the WCO to meet the KO at the desired point. The WCO is not affected very much by the sun and its closest distance to the sun will be 7.042×10^{12} m.

Figure 1-C and Table 2 show the different orbits such an encounter can produce. All these orbits are closed and in the same rotation as the initial object, counter-clockwise. The initial orbit is the dotted black ellipse in the center of the figure. We use the same colour code as before to show the decrease-increase in the impact parameter between the CWO and the KO. When the impact parameter is large, not much happens and as the impact parameter decreases, the orbit is perturbed and produces the large orbits represented in red. As

the impact parameter decreases the KO is ejected in outer space before being deflected toward the sun and again ejected from the solar system. Then, the deflection toward the sun produces closed but very elongated orbits in dotted green, blue and magenta ellipses. As the impact parameter continues to increase, the collision produces less eccentric orbits (light blue and black) until the orbit is perturbed very little. It is important to note here that the highly eccentric orbits are produced by sending the KO first toward the sun. There is a window of impact parameters that will send the KO out of the solar system either by sending them first toward the sun or directly into outer space.

Exit point, D

Figure 1-D and Table 2 show the different orbits that we can obtain when the WCO exits crosses the orbit of a KO as it moves out. The structure is a little simpler here: as the impact parameter decreases, the orbit is pulled down and amplified (red) until it reaches very large aphelion (green). Then, the impact parameter decreases some more and the KO is sent toward the sun before being ejected from the solar system. As the impact parameter increases a little, the KO is sent to outer space on long, highly eccentric orbits (dotted blue and magenta) Finally, as the impact parameter increases, the orbits settle on less eccentric orbits that will be closer and closer to the original orbits. In this figure, all orbits have the same rotation as the original orbit (counter-clockwise). One must note here that in this collision process, it has been impossible to send the original KO toward the sun and obtain a closed orbit. All orbits that send the KO toward the sun eject the KO from the solar system. One must also note that the range of values for q to produce long, eccentric orbits is rather small (dotted blue and magenta) Again, such collisions cannot produce a perturbed orbit where $q > Q_K$.

We also note clustering of the EKO-I and EKO-II. The clustering is a little different depending whether we have a head-on encounter or a rear-end encounter. The EKO-I will be more back-to-back in a head-on encounter than in a rear-end encounter: about 170 degrees vs about 140 degrees in our case. The EKO-II will be less back to back in a head-on collision than in a rear-end collision: about 120 degrees vs about 140 degrees in our case.

Discussion

We see that both types of orbits (EKO-I and EKO-II or Class-I and Class-II) are produced in the collision process. There is however a difference in their respective windows: the window to produce EKO-I is larger than that to produce EKO-II. Furthermore, there is also a difference in the range of values allowed for q in an EKO-II orbit depending whether we have a head on collision or a rear end collision: the range is smaller when the perturbed orbit is produced at the exit point in a rear end collision.

Regarding the clustering, we note that EKO-I are produced on the opposite side of the trajectory of the CWO with respect to the sun while the EKO-II are produced on the same side. This clearly means that the passage of a single CWO through the edge of the Kuiper belt would produce several objects of

EKO-I and EKO-II classes that would not be uniformly distributed around the sun: each class would be produced on one side of the sun or the other. Such clustering has been observed before as resulting from the influence of NP [de la Fuente Marcos, 2017; Batygin, 2016b] as well as comets [Rickman et al., 2001]

In the previous encounters, the CWO stays far from the sun and its path is not affected much: it will suffer a deviation of about a degree (or less). Its path is almost a straight line that is about perpendicular to the bisector of the angle between the two clusters (entrance and exit), both for EKO-I and EKO-II. Furthermore, as the orbits of the EKO are stable, it is very difficult to estimate when this encounter took place. From the positions of the objects discovered up to now on their respective orbit, it could be possible to estimate the number of cycles they have performed if we assume that they were produced at about the same time since the WCO crosses our solar system in a relatively short period.

There is also a recurrent pattern to be noticed: for both EKO-I and EKO-II produced in this process, when q decreases, Q increases. This holds as long as the EKO-I and EKO-II produced originate from the same initial KO, the only difference being where the CWO interacts with the KO on its orbit. If we allow for the initial KO orbit to vary (q, Q, θ_x), this relation will not quite hold when we compare the different EKO produced. If the initial parameters of the different KO are similar, the relation should hold relatively well.

Grazing collision

We have studied a collision where the WCO cuts slightly the Kuiper belt. As the collision becomes more and more grazing, (points A and B, or C and D get closer) the window to produce EKO-II decreases and the range in q will also become very small. Eventually, when the collision is almost tangential, it will be impossible to produce EKO-II while it will always be possible to produce EKO-I orbits. In that configuration, all objects sent towards the sun are ejected from the solar system, there is no stable EKO-II orbit.

Second Encounter

Since the previous encounter cannot produce an orbit where $q > Q_{kuiper}^{original}$ and several of these objects have been observed (Class-III objects) we will allow the WCO to intersect the orbit of a typical EKO-I: $q_{EKO-I} = 6.4 \times 10^{12}m$ and $Q_{EKO-I} = 5.67 \times 10^{13}m$, which leads to $\varepsilon = 0.797$. We will let the distance from the sun (x , since the sun is at the origin) vary from 3×10^{13} to 5×10^{13} ; the y coordinate being dictated by the original KO trajectory. The speed of the CWO will be $(0, 50000)m/sec$, as before. The CWO is affected by the sun, but very little; its deflection being about 1 degree. For example, when it starts at $x = -5 \times 10^{13}m$, its closest distance to the sun will be about $-4.99 \times 10^{13}m$. Of course, the impact parameter between the CWO and the KO is much smaller. Figure 2 and Table 3 show orbits that such encounters can produce; the original orbit is the little ellipse at the center. The larger orbit is similar to 2015TG387, the second one is similar to 2013SY99, the third one is similar to 2003VB12 (Sedna) and the fourth one is similar to 2012VP113; these are the FKO-I. We also show another interesting orbit that is very large, has a relatively

small eccentricity and runs clockwise; this is the FKO-II.. It is important to note that in order to produce 2003VP113, the CWO came from the lower right such that its initial velocity was $(-25.0, 25.0)$ km/sec so that its velocity is about 35 km/sec as opposed to the usual 50 km/sec. This produced the desired orbit while staying far enough from the sun (at least 80 AU) so as to not disturb the Kuiper belt. Similarly, in order to produce the clockwise rotating orbit, the initial velocity of the CWO was $(-25.0, 40.0)$ km/sec which allowed it to stay far from the sun (at least 80 AU). One can see a pattern in the production of the FKO-I: when the interaction CWO-EKOI takes place closer to the sun, it will have a tendency to produce FKO-I with larger values of q . For similar values of q there is a fair range of values for Q by adjusting the collision parameters since all these encounters can eject the EKO-I when the CWO gets too close to the KO.

In order to produce the four FKO-I, a single WCO would have to cross the paths of four EKO-I. This scenario seems unlikely, but one can also take the point of view that if a first WCO produced several EKO-I, then a second object could cross their paths and produce something. In this view, the configuration that we have now is just one among several possibilities. The precise configuration of these 4 objects will depend where the CWO crossed the original EKO-I orbits and their orientation. The orbits that we present on Figure 2 do not reproduce exactly those of these 4 objects because all three were produced from close points on the orbit of the original EKO-I. One can imagine however that these orbits can be reproduced in their configuration by allowing the CWO to cross the four EKO-I at different point on their respective orbit.

One must keep in mind also that the passage of a CWO in the neighbourhood of an FKO-I can realign its orbit by as much as 30-40 degrees, while leaving the other orbital parameters (q, Q) relatively unchanged. This way, a CWO passing relatively close to 2015TG387 when it is close to its aphelion could have modified its orientation while leaving Sedna and 2012VP113 unchanged; it might also have left 2013SY99 unchanged, depending where it was on its orbit.

On Figure 3 and Table 4, we present some orbits that can be produced by the encounter of a WCO with an EKO-II. The EKO-II can remain in this class but its spin can be inverted. It can also become an EKO-I and again both spin directions are possible. It seems very difficult however to bring it back to a simple KO. Finally, it is possible to send it on very large orbits with relatively small eccentricities where both spinning directions are possible. These are the FKO-III class and they can be likened to the Lower Oort Cloud objects as their Q becomes a fair fraction of a light year.

Two and three dimensions

We have worked exclusively in two dimensions (2D) and one could argue that we have not reproduced all the orbits of the Sednitos discovered over the past 20 years; the most spectacular example being 2015BP519 which sticks out of the general orbital plane at 57 degrees or so. This poses a problem as Brassier et al. (2012) have shown that scattering interactions with the giant planets do not rise the orbital inclinations by much. As mentioned previously, this peculiar orbit

could have been produced by NP but caution is required in this interpretation. However, as we have seen, the final orbital parameters of the perturbed objects depend greatly on the precise parameters of the encounter between the WCO and the initial object. No doubt that a slight difference in the encounter can have huge impact on the final parameters. For example, were the WCO to cross the orbital plane of the Kuiper belt instead of moving within it, this would have huge impacts and could very easily project the KO in an orbit perpendicular to the Kuiperian plane. Clearly, adding the third dimension complicates the problem substantially and we are confident that the main results provided in this paper would be valid in 3D. There is also an interesting mechanism discovered by Madigan [Madigan & McCout, 2016, Madigan et al. 2018] called *inclination instability* where several eccentric orbits drive exponentially their inclination with respect to the solar plane. This process could potentially explain the very large inclination of 2015BP519.

Mass, speed and zone of influence

In this work, we have set the mass of the messenger at 0.1 solar mass. In this way, it is barely a star and could have eluded detection up to now. We have verified that the zone of influence of this object on the Kuiper Belt is about 10 AUs in the sense that when the distance between the KO and the CWO is more than 10 AUs, the orbital parameters of the KO (q and Q) will remain within 10% of their initial values, which means that it will remain as a standard KO. This definition is not as constraining as that of Gladman et al. (2008) regarding scattering objects but it seems reasonable for our purposes. If the KO object has a slightly eccentric orbit, the axes of the ellipse can be rotated by up to 90 degrees in some collisions, but the parameters will remain within 10% of their initial values. Clearly, by reducing the mass of the CWO, that radius of the zone of influence will diminish, but so will the cross-section of interaction with the objects: the CWO will have to get closer to the KO in order to eject it out of the solar system or promote it to higher orbits.

The speed of the KO could also have an impact on the possibility of ejecting a KO out of the solar system or promoting it to higher orbits. This is another relatively free parameter that makes the prediction of the location of the CWO very difficult; we can estimate its direction from the clusters its passage has produced.

We have verified that the angle between the clusters (EKO-I or EKO-II) gets smaller (they become less back-to-back) as the collision between the CWO and the KO is moved farther away from the sun; it is about 140 degrees when the encounter takes place at about 80 AU, as opposed to about 170 degrees at 55 AU.

Scenario

When we take into account the following:

- Scholz star has been observed and there might be more such objects

- several EKO-II (or Class-II) objects have been discovered so far and their window of production is small and vanishes as the collision WCO-KO becomes tangential
- several FKO-I (or Class-III) objects have been discovered so far and the production of a single FKO-I requires the interaction of a CWO with an EKO-I
- the production of several FKO-I through the passage of a single CWO seems unlikely and the passages of several WCO that would each produce a FKO-I seems also unlikely
- clustering has been observed among the ETNO and clustering occurs naturally through the passage of a WCO across the out-skirt of the Kuiper Belt
- the angle between clusters decreases as the point of interaction between the CWO and the KO is moved farther away from the sun (80 AU for example)
- the FKO-I (or Class-III) objects observed up to now respect relatively well the relation observed here that when q decreases, Q increases
- the range of influence of a 0.1 solar mass CWO is about 10 AU

we are lead to consider the possibility that the Kuiper Belt might have been substantially larger than what it is now. In this scenario, a CWO would have cut through the out-skirt of this extended Kuiper belt. This would have depleted the belt of several members that would have been ejected but it would have also produced several objects in the EKO-I and EKO-II classes. The FKO-I (or Class-III) objects that are so difficult to produce from the actual Kuiper belt, would simply be EKO-I of the encounter CWO – KO^{extended}. There could be one or two of these encounters, potentially over very long periods of time since the orbits are stable, on the same side of the sun or on opposite sides of the sun. Such a process likely would also create objects in classes that have not been observed yet; counter-rotating objects with very large semi-major axis and relatively small eccentricity for example. The resulting Kuiper belt would not be symmetric anymore and the asymmetrical bulges (sections of the belt that were left more or less untouched by the passages of the CWO) could be brought back in line with the belt by the gravitational forces of the belt over a long period of time. This scenario offers the beginning of a process where the Kuiper belt would eventually build a cut-off at about 50 AU.

Interestingly, the *inclination instability* among eccentric orbits discovered by Madigan requires a large population of small objects beyond 50 AU and a few thousands AU with a total mass of 1-10 Earth masses to be able to operate. If this scenario is correct, the passage of a WCO at about 90 AU could have produced several exotic objects if the number of these objects is sufficiently large to make several encounters probable.

Clearly, if we want to consider an extended Kuiper Belt in this scenario, its width would have to be at least equal to the largest $q^{Class-III}$ which is about 80 AU. Furthermore, considering the EKO-II elements (mainly 2005VX3, 2012DR30, 2015ER61, and 2013BL76) one can see that there isn't half a plane that is not covered, which would indicate that there has been at least two WCO encounters, at least one on each side of the sun. Depending on how one combines these EKO-II into pairs, several orientations of the CWO would be possible. The clusterings might not be all that clear due to the different initial orbital parameters (q, Q, θ_x) of the different KO affected in the process. This might also explain why the four Class-III objects listed in Table 1 do not respect the relation that when q decreases, Q increases: three elements respect this relation but a fourth one does not. This could mean that three elements had relatively close orbital parameters while the fourth one did not.

Consider now the clusterings presented on Figure 4 of Sheppard & Trujillo (2019) (figure 1 of Batygin & Morbidelli (2019) is similar) to which we add 2015ER61, 2017DR30, 2015VX3 and 2013BL76. The main clustering presents two lobes consistent with what we have presented here; these would be EKO-I of an encounter CWO – KO^{extended} where the trajectory of the CWO would have been about perpendicular to the major axis of the Distant Eccentric Planet indicated on Figure 4. However, when we add 2015ER61 and 2017DR30 we run into a problem because the EKO-II are more back-to-back than the EKO-I, which is contrary to what we have seen here. Another possibility is to consider one lobe aligned roughly with 2012VP113, another lobe aligned with the secondary cluster together with 2017DR30 and 2015VX3. This pattern could arise from the passage of a CWO with a trajectory at about 45 degrees with the major axis of the Distant Eccentric Planet. A second CWO parallel to the first one could explain 2015ER61, 2013BL76 and a lobe aligned roughly with Sedna but there would be a lobe missing between the Secondary cluster and 2017DR30. Of course, if the CWO does not encounter any KO susceptible to produce an EKO-I, there could be a lobe missing. Clearly, there are several possibilities and a full simulation involving hundreds or thousands of KO with a random angular distribution but a tapering-off radial distribution extending up to 90-100 AU and being the target of a CWO that would slice through it at about 85 AU would be very interesting !

Lastly, it is worth mentioning that it is possible to produce FKO-III, similar to those one could expect from a lower Oort cloud object (LOCO) not by interacting with the FKO-II itself, but with the sun. This is essentially conservation of angular momentum; it is shown on Figure 4 and Table 4 where the original path of the FKO-II is the small ellipse at the center; it spins counter-clockwise. The CWO is closest to the sun when the FKO-II is at the point where its orbit changes; close to its aphelion. The path where the CWO is deflected clockwise with respect to its original direction produces the FKO that rotates clockwise (red orbit) since the sun will acquire a counter-clockwise angular momentum in this collision. Conversely, the path where the Cosmic Messenger is deflected counter-clockwise with respect to its original direction produces the FKO that rotates counter-clockwise (green orbit), the same rotation as the original orbit,

but with a much larger aphelion. Note that in both cases, the FKO is very far from the CWO and the sun when these two collide and the minimal distance between the CWO and the FKO-II is comparable to that between the sun and the FKO-II at the moment of the collision. Clearly, such an encounter would wreak havoc within the inner solar system and such effects would be seen on the motion of the inner planets.

Conclusions

We have studied the effects of the passage of a light WCO intersecting the outer edge of our Kuiper belt. We have set the mass of the WCO at 10% of a solar mass so that it is barely a star and practically invisible.

We have seen that a WCO that crosses the orbit of a KO can eject it from the solar system, but it can also send it on two different types of orbits: EKO-I that have perihelions similar to but smaller than $Q_{initial}^{Kuiper}$ and EKO-II whose perihelion is much smaller and can be just a few AU. EKO-I have a wider range of eccentricities while EKO-II tend to have very large eccentricities. Both will be produced in clusters and will obey the rule that if q decreases, Q increases. It is impossible to produce an orbit such that $q_{new} > Q_{initial}^{Kuiper}$. We have seen that objects like Sedna can be produced through the interaction of a CWO with an EKO-I object. However, considering the fact that each Sedna requires the interaction of a CWO with an EKO-I, it seems very unlikely that several CWO would have produced the Sednas that we have observed up to now. Instead, it seems more appealing to consider the scenario where the Kuiper Belt was larger than what it is now, maybe not uniformed either so that current Sednas are in fact EKO-I of an encounter between a CWO and an extended Kuiper belt. Most of the Sednas observed up to now respect the rule that when q increases, Q decreases, indicating that the original KO orbits were fairly close to each other. The process studied here has a tendency to produce objects in clusters and the angle between the clusters decreases as the point of interaction CWO-KO moves farther away from the sun. These observations point to an interaction that took place farther than 50 AU. This would require the extended Kuiper belt to reach about 90-100 AU and the encounter between the CWO and the KO to take place at about 85 AU. Furthermore, considering the current EKO-II population where much less than half of the plane is unoccupied, this mechanism would require at least two WCO, at least one on each side of the sun, to interact with the out-skirt of the extended Kuiper Belt. The scenario where a CWO skims an extended Kuiper Belt offers also the beginning of a mechanism that would eventually produce a sharp edge to the remaining Kuiper Belt.

The same way that the passage of Scholz's star seems to have left some traces in the radiants that have been observed, it is likely that the passage of a few CWO would also leave traces in the radiants, even though the mass that we used here for our CWO is less than that of Scholz's system.

Acknowledgements

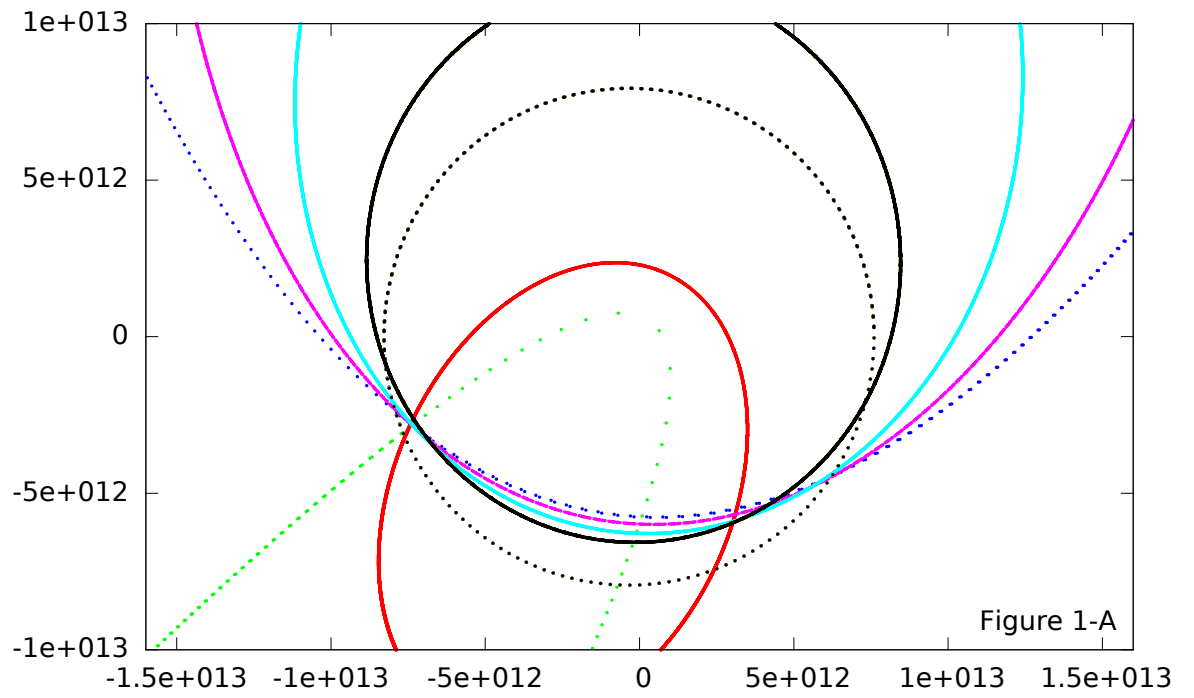
I want to thank my colleague C. Hamzaoui for interesting, enjoyable and stim-

ulating discussions and G. Hellou for comments on the manuscript. I also want to thank my colleagues from the Atlas Collaboration at the physics department at Université de Montréal for the use of their computers.

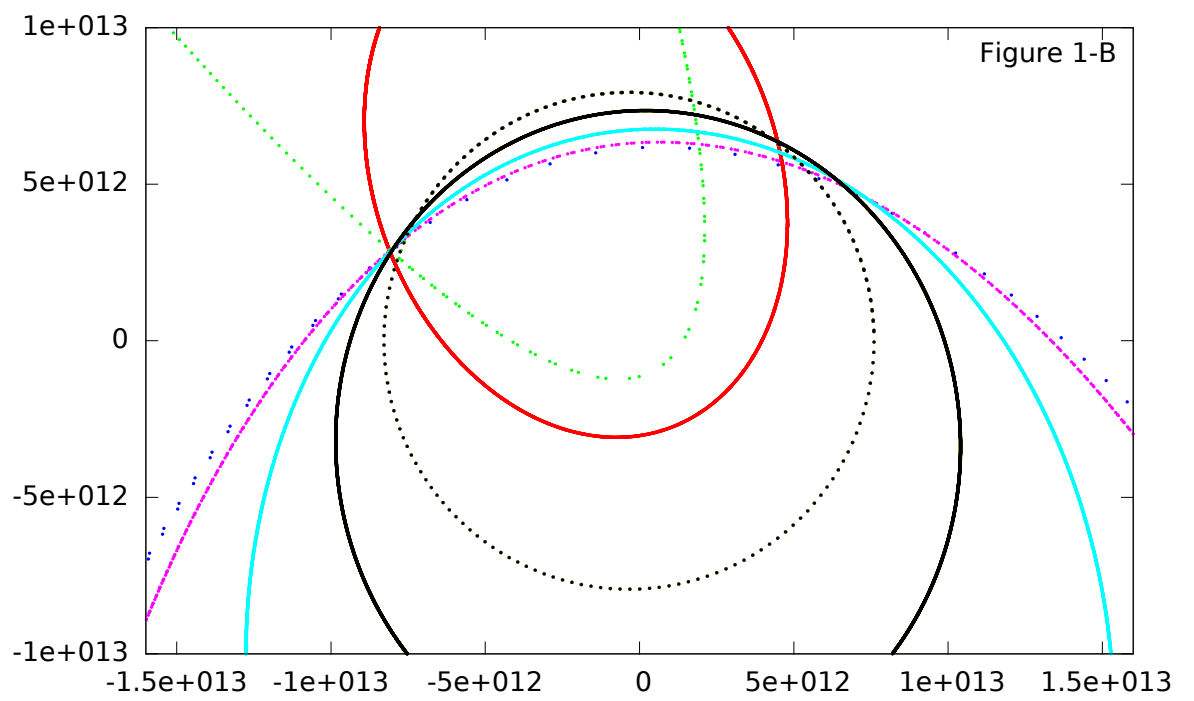
References

- Allen, R.L., Bernstein, G.M., Malhotra, R., *ApJ*, 549, L241-L-244 (2001)
- Bacci, P., Maestripieri, M., Tesi, L. *et al.*, 2017, MPEC 2017-U181
- Bannister, M.T., Shankman, C., Volk, K., *et al.*, 2017, arXiv:1704.01952v1[astro-ph.EP]
- Bannister, M.T., Schwamb, M., Fraser, W.C., *et al.*, 2017b, *ApJ*, 851, L38
- Bannister, M.T., Alexandersen, M., Benecchi, S.D. *et al.* 2016, **AJ**, 152:212
- Batygin, K., Brown, M.E.; 2016, *AJ*, 151, 22
- Batygin, K., Brown, M.E.; 2016b, *ApJ*, 833, L3
- Batygin, K., Morbidelli, A., 2017, arXiv:1710.01804v1[astro-ph.EP]
- Becker, J.C., Khain, T., Hamilton, S.J., *et al.*, 2018, *AJ*, 156, 2
- Brasser, R., Schwamb, M.E., Lykawka, P.S., & Gomes, R.S. 2012, *MNRAS*, 420, 3396
- Brasser, R., Schwamb, M., *MNRAS*, 446, 3788, 2015
- Brasser, R., Morbidelli, A., 2013, *Icarus*, 225, pp 40-49
- Brasser, R., Duncan, M.J., Levison, H.F., Schwamb, M.E., Brown, M.E., 2012, *Icarus*, 217, 1-19
- Bromley, B.C., Kenyon, S.J., 2016, *ApJ*, 826, 64
- Brown, M.E., Trujillo, C., Rabinowitz, D., 2004; *ApJ*, 617, 589-599
- Fernandez, J.A., Brunini, A., *Icarus* 106, 580-590 (2000)
- Fraser, W.C., Bannister, M.T., Pike, R.E. *et als*, 2017, *Nature-Astronomy*, 1, 0088
- de la Fuente Marcos, C., R. de la Fuente Marcos, Aarseth, S.J., 2018; *MNRAS*, 476, (1), L1-L5
- de la Fuente Marcos, C., R. de la Fuente Marcos, 2018b, *RNAAS*, 2 2018
- de la Fuente Marcos, C., R. de la Fuente Marcos, 2017; *MNRAS*, 471, (1), L61-L65
- de la Fuente Marcos, C., de la Fuente Marcos, R., 2014, *MNRAS*, 443, L59
- Fienga, A., Laskar, J., Manche, H., Gastineau, M., 2016; *A&A*, 587, L8
- Gladman, B., Kavelaars, J.J., Petit, J.-M., Morbidelli, A., Holman, M.J., Lored, T., 2001, *AJ*, 122, 1051-1066
- Gladman, B., Holman, M., Grav, T. *et al.*, 2002, *Icarus*, 157, 269-279
- Gladman, B., Marsden, B. G., Vanlaerhoven, C., *Nomenclature in the Outer Solar System*, ed. M.A. Barucci, H. Boehnhardt, D. P. Cruikshank, A. Morbidelli, Dotson, R., 43-57, 2008
- Gomes, R.S. 2003, *Icarus*, 161, 404-418
- Gomes, R., Fernandez, J., Gallardo, T., Mrumini, A., 2008, *The Solar System beyond Neptune* ed. M. Barucci et al., (Tucson, AZ., Univ. Arizona Press), pp 259-273
- Hands, T.O., Dehnen, W., Gration, A., Stadel, J., Moore, B., 2019, *MNRAS* april
- Holman, M.J., Payne, M.J., Fraser, W., *et al.*, 2018, *ApJ*, 855, L6
- Ida, S., Larwood, J., Burkert, A., 2000, *ApJ*, 528, 351-356
- Jilkova, L., Portegies Zwart, S., Tjibaria, P., Hammer, M.; 2015, *MNRAS*, 453, (3), 3157

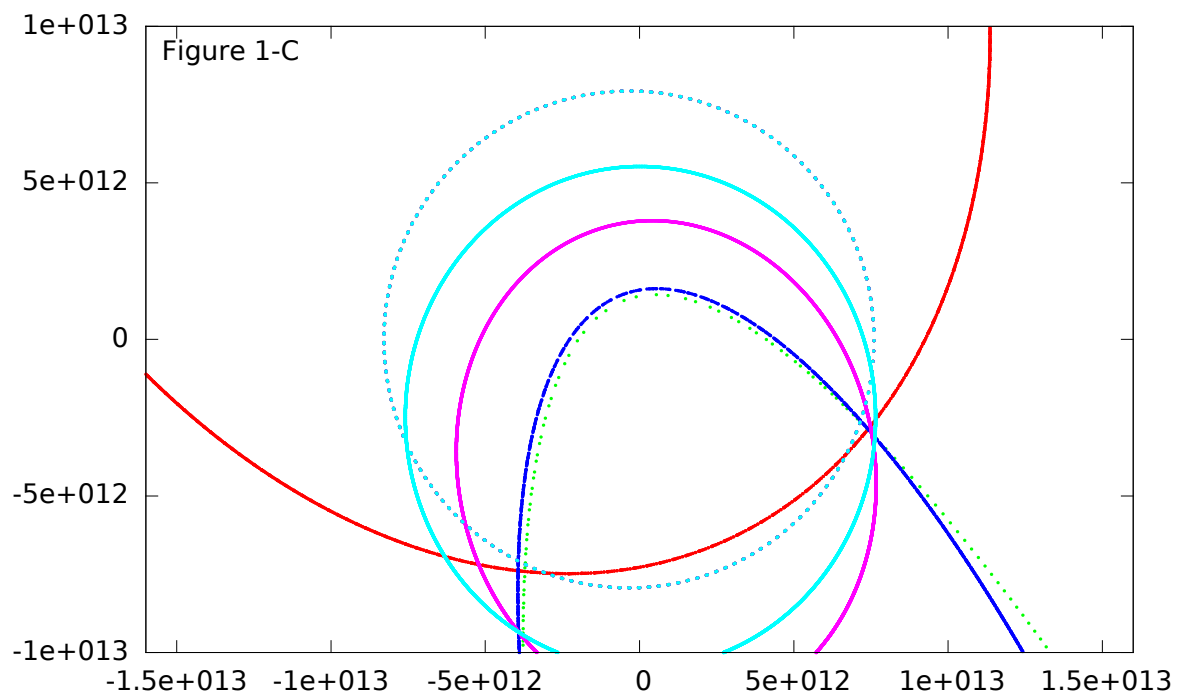
Kaib,N.A.,Pike,R.,Lawler,S.,*et al.*,2019,arXiv:1905-09286v2[astro-ph.EP]
 Kenyon,S.J.,Bromly,B.C.,2004, *Nature*,*432*, 598-602
 Knight, M.M.,Protopapa, S., Kelley, S.S.P., et al., 2017,*ApJ*,*851*, L31
 Lawler,S.M.,Shankman,C.,Kaib,N., *et al.*,2016,*AJ*,*153*, 1
 Levison, H.F., Morbidelli,A.,van Laerhoven, C.,Gomes,R.,2007,
Icarus,*196*, 258-273
 Li,G.,Adams,F.C.,2016,*ApJ*,*823*,L3.
 Linder,E.F.,Mordasini,C.,2016;*A&A*,*589*,A134
 Madigan, A.-M., McCourt, M.,2016,*MNRAS*,*457*, L89
 Madigan,A.-M., Zderic, A.,McCourt,M., Fleisig, J.,2018, *AJ*,*156*,4
 Malhotra, R.,Volk,K.,Wang,X.,2016;*A&A*,*589*,A134
 Mamajek,E.E.,Barenfeld,S.S.,Ivanov,V.D.,Kniazhev,A.Y.,Vaisanen,P.,
 Beletsky,Y.,Boffin,H.M.J.,2015,*ApJ*,*800*,L17
 Meech,K.,Bacci,P.,Maestriperieri,M.,*et al.*,2017,*MPEC 2017-U183.A/2017 U1*
 Meech, K.J., et al. 2017b, *Nature*,*552*, 378
 Millholland,S.,Laughlin,G.,2017,*AJ*,*153*,91
 Morbidelli, A., Emel'yanenko,V., Levison, H.F.,2004, *MNRAS*,*355*,935-940
 Morbidelli, A.,Nesvorny,D.; 2019 arXiv:1904.02980v1[astro-ph.EP]
 Morbidelli, A.,Levison,H.F.,2004,*ApJ*,*128*,2564
 Morbidelli, A.,Levison, H.F., Gomes, R, 2007 arXiv:astro-ph/07-3558v1
 Pfalzner,S.,Bannister,M.T.,2019, *ApJ*, *874*,L34
 Rickman, H.,Valsecchi, G.B., Froeschl, C., 2001,*MNRAS*,*325*, 1303
 Scholz,R.-D.,2014,*A&A*,*561*,A113
 Shankman,C.,Kavelaars,J.J.,Bannister,M.T.,Gladman,B.J.,Lawler,S.M.,
 Chen,Y.-T.,Jakubik,M.,Kaib,N.,Alexandersen,M.,Gwyn,S.D.J.,
 Petit,J.-M., Volk,K.,2017, *AJ* *154*, 50
 Sheppard,S.S.,Trujillo, C., Tholen,D.J,2016, *ApJ*,*825*, L13
 Sheppard,S.S.,Trujillo,C.A.,2016b, *AJ*,*152*, 221
 Sheppard, S.S.,Trujillo,C.A.,Tholen,D.J.,Kaib,N.,2019, *AJ*,*157*,139
 Singer,K.N.,McKinnon,W.B.,Gladman,B.,*et al.*, 2019, *Science*,*363*,955
 Stern,S.A.,2004, arXiv:astro-ph/0404525v2
 Thirouin,A.,Sheppard,S.S.,2018;arXiv:1804.09695v1[astro-ph.EP]
 Thirouin,A.,Sheppard,S.S.,Noll,K.S.,2017;*ApJ*,*844*,135
 Trujillo, C.A., Brown, M.E., 2001,*AJ*, *554*, L95-L98
 Trujillo,C.A.,Sheppard,S.S., 2014,*Nature*,*507*,471



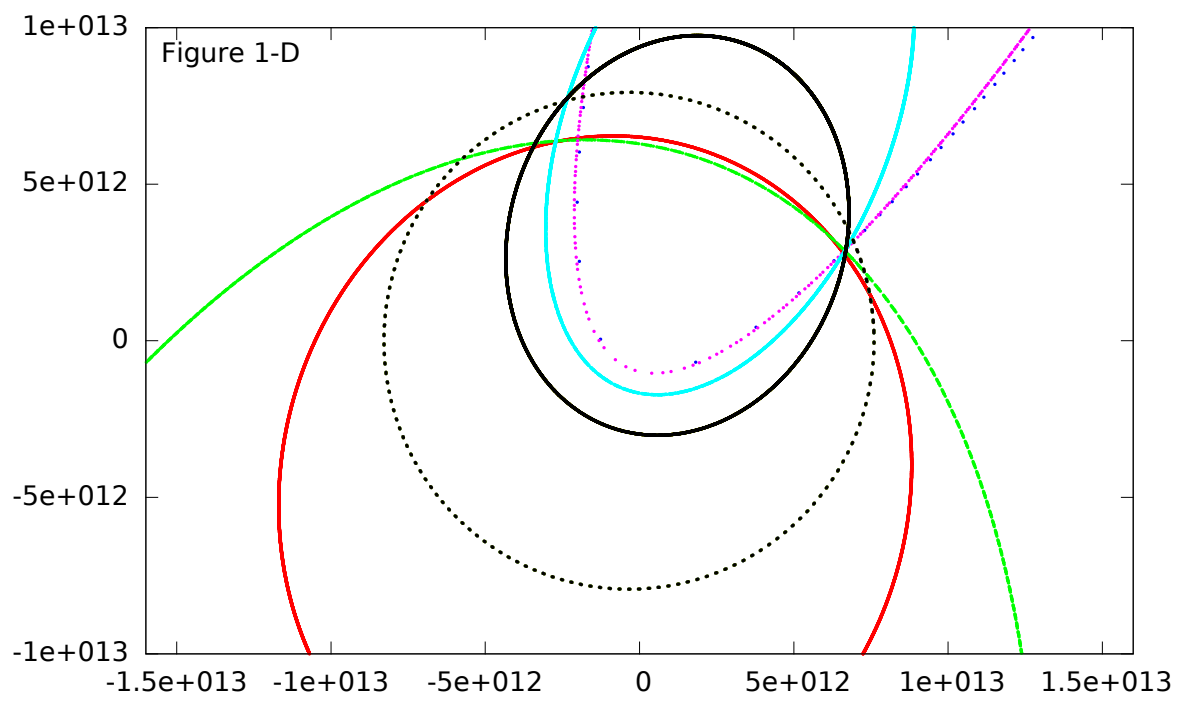
Orbits produced at the entrance in a head-on collision between a CWO and a KO.

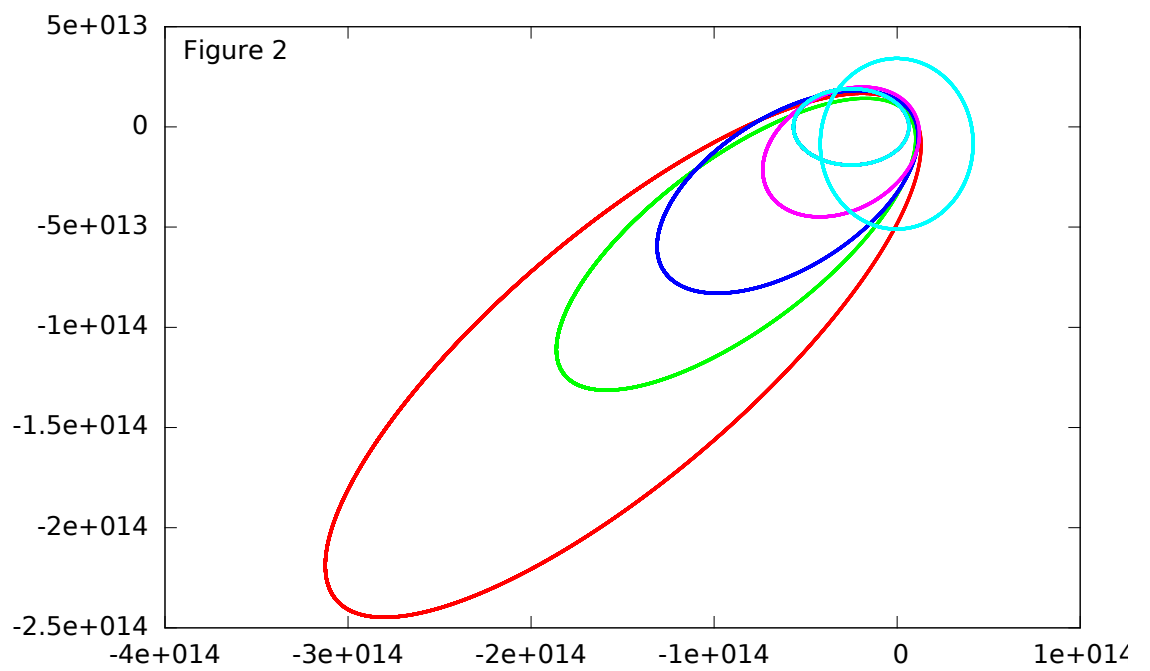


Orbits produced at the exit in a head-on collision between a CWO and a KO.

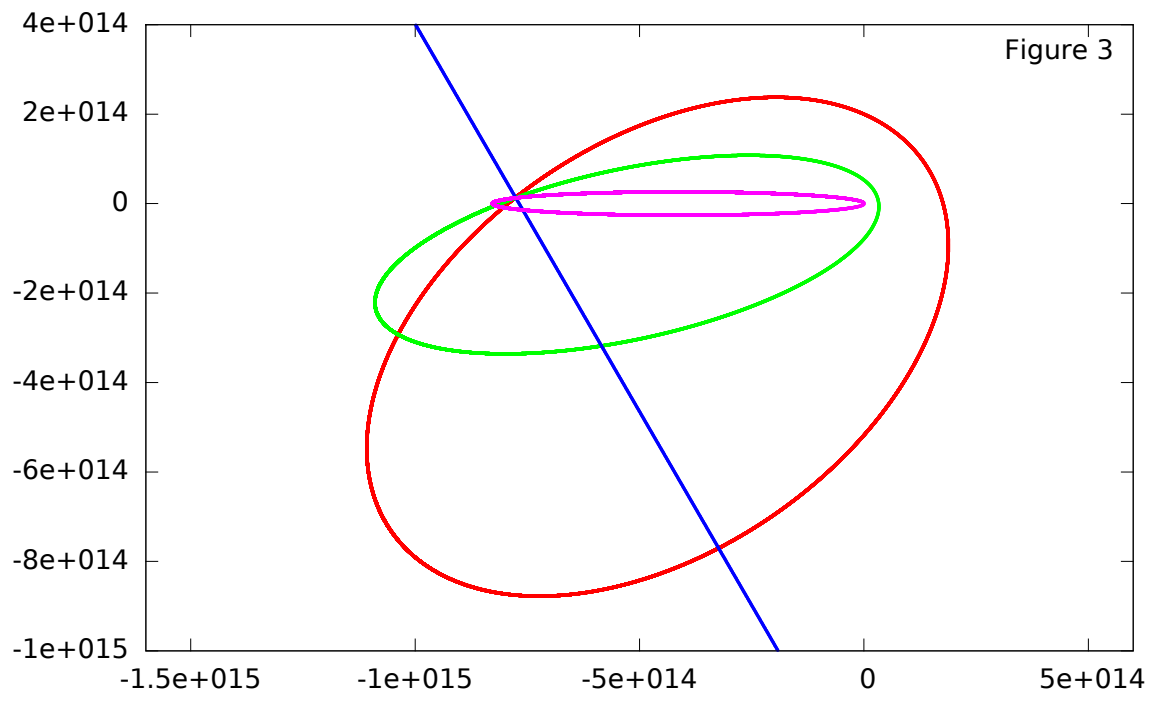


Orbits produced at the entrance of a rear-end collision between a CWO and a KO.

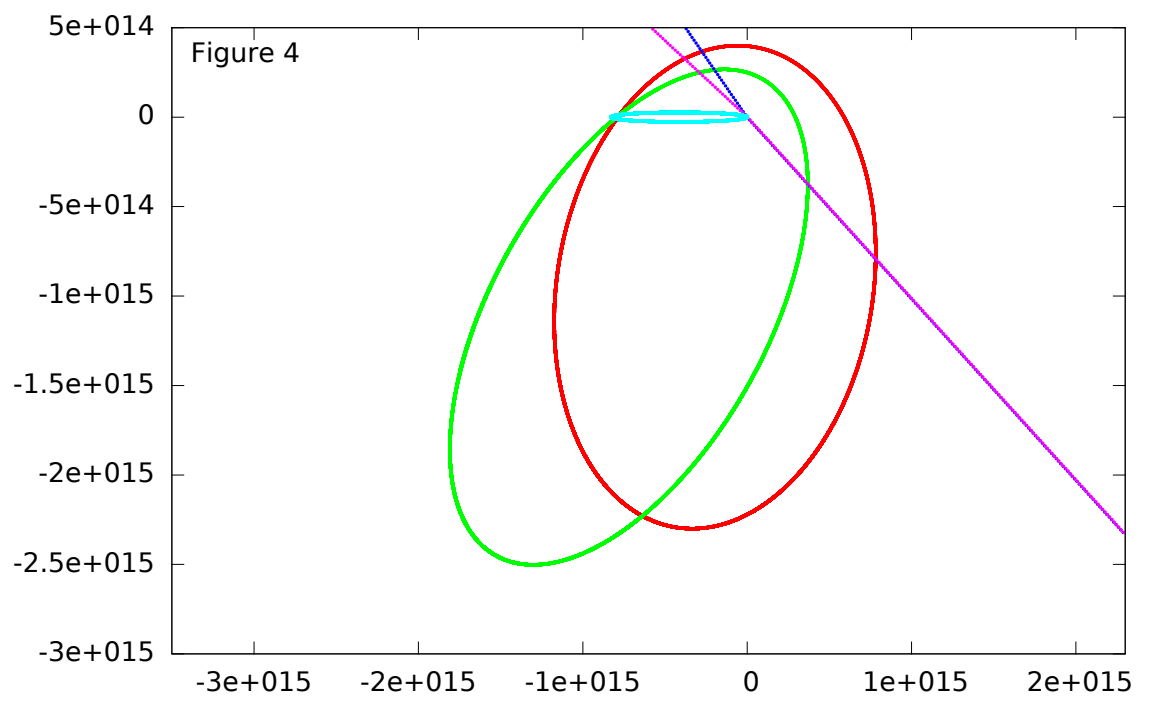




Orbits produced in the collision between a CWO and an EKO-I that reproduce 4 known exotic objects.



Orbits produced in the collision between a CWO and an EKO-II.



Orbits produced from an EKO-II in the collision between a CWO and the Sun.

Table 1: Orbital parameters of known objects

Element	q(AU)	Q(AU)
Class I		
2004VN112	47.3	585
2014FZ71	56	97
2013RF98	36	662
2000OO67	20	1068
2006SQ372	24.1	1461
2013FY27	37	82
2015BP519	35	824
2015KG163	40	1581
2015GT50	38	631
2014FE72	36	3850
2014SR349	47	535
Class II		
2005VX3	4.13	3079
2002RN109	2.7	1155
2013BL76	8.36	2151
2010BK118	6.1	963
2010NV1	9.3	596
2015ER61	1.06	2487
2007DA61	2.67	990
2013AZ60	7.92	1117
2012DR30	14.6	2939
Class III		
2003VB12	76	954
2012VP113	80.5	445
2015TG387	65	2275
2013SY99	50	1420

this list is not exhaustive
but representative

Table 2: Orbital parameters

Element	$q(\frac{m}{AU})$	$Q(\frac{m}{AU})$	θ_x^Q
Figure 1			
initial	7.60×10^{12} 50	8.28×10^{12} 55.2	180
Figure 1-A			
red	2.18×10^{12} 14.5	1.35×10^{13} 89.3	-115
green	5.79×10^{11} 3.9	1.91×10^{15} 12733	-127
blue	5.72×10^{12} 38.1	1.36×10^{15} 9067	+84
magenta	5.96×10^{12} 39.7	5.20×10^{13} 347	+85
light blue	6.26×10^{12} 41.7	2.21×10^{13} 147	+85
black	6.57×10^{12} 43.8	1.14×10^{13} 76	+87
Figure 1-B			
red	2.95×10^{12} 19.7	1.45×10^{13} 96.7	+109
green	1.06×10^{12} 7.1	2.51×10^{14} 1673	+120
blue	6.13×10^{12} 40.9	1.93×10^{15} 12867	-84
magenta	6.28×10^{12} 41.9	1.19×10^{14} 793	-83
light blue	6.75×10^{12} 45	2.93×10^{13} 195	-82
black	7.35×10^{12} 49	1.39×10^{13} 92.7	-88
Figure 1-C			
red	7.00×10^{12} 46.7	4.21×10^{13} 281	+115
green	1.34×10^{12} 8.9	8.01×10^{13} 5340	-70
blue	1.53×10^{12} 10.2	6.44×10^{13} 429	-70
magenta	3.75×10^{12} 25	1.21×10^{13} 80.7	-78
light blue	5.52×10^{12} 36.8	1.05×10^{13} 70	-90
Figure 1-D			
red	6.41×10^{12} 42.7	1.61×10^{13} 107	-109
green	6.16×10^{12} 41.1	6.74×10^{13} 449	-107
blue	8.88×10^{11} 5.9	8.39×10^{13} 5593	+64
magenta	9.49×10^{11} 6.3	1.36×10^{14} 907	+65
light blue	1.62×10^{12} 10.8	1.68×10^{13} 112	+67
black	2.92×10^{12} 19.2	1.01×10^{13} 67.3	+70

Table 3: Orbital parameters

Element	$q(\frac{m}{AU})$	$Q(\frac{m}{AU})$	\pm	$x_{interaction}(m)$
Figure 2				
initial	6.40×10^{12} 42.7	5.66×10^{12} 377	+	****
red	1.05×10^{13} 70	3.86×10^{14} 2576	+	-5.0×10^{13}
green	8.50×10^{12} 57	2.19×10^{14} 1462	+	-5.5×10^{13}
blue	1.03×10^{13} 69	1.45×10^{14} 968	+	-4.5×10^{13}
magenta	1.17×10^{13} 78	7.74×10^{13} 516	+	-3.0×10^{13}
light blue	3.42×10^{13} 228	5.10×10^{13} 340	-	-3.3×10^{13}

+ is counterclockwise rotation

- is clockwise rotation

Table 4: Orbital parameters

Element	$q(\frac{m}{AU})$	$Q(\frac{m}{AU})$	\pm
Figure 3			
initial	8.3×10^{11} 5.53	8.28×10^{14} 5520	+
red	1.63×10^{14}	1.28×10^{15} 8533	+
green	3.26×10^{13} 217	1.11×10^{15} 7400	-
Figure 4			
initial	8.3×10^{11} 5.53	8.28×10^{14} 5520	+
red	3.81×10^{14} 2540	2.38×10^{15} 15867	-
green	2.22×10^{14} 1480	2.92×10^{15} 19467	+

+ is counterclockwise rotation

- is clockwise rotation